A HIGH-ORDER-MODULATION SPACE-TIME RECEIVER WITH INCREASED PEAK RATE AND THROUGHPUT FOR WIDEBAND CDMA

Sofiène Affes, Karim Cheikhrouhou, Faker Moatemri, Khaled Lajnef, and Paul Mermelstein

INRS-ÉMT, Université du Québec
800, de la Gauchetière West, Suite 6900, Montreal, Quebec, Canada
{affes,cheikhro,moatemri,lajnef,mermel}@emt.inrs.ca

ABSTRACT

In this work, we significantly increase the peak rate of the wideband CDMA spatio-temporal array-receiver (STAR) by enabling its operation with high-order modulations (HOM) up to 256QAM (i.e., peak rate of 768 Kb/s per spreading code with 32 spreading factor and 1/2 coding rate in 5 MHz). In order to allow an effective rate control for adaptive modulation and maximize throughput with the resulting HOM-STAR, we propose the use of power control (PC) jointly with new rate allocation schemes (RAS). At a load of 20 users per cell or sector, simulations suggest that HOM-STAR with the new RAS can deliver an average throughput per user of 120-140 Kb/s, i.e., an increase of about 100% over conventional RAS.

1. INTRODUCTION

Recent deployments of 3G networks are currently allowing transmission rates hardly reaching the peak rates of 384 Kb/s and 2 Mb/s targeted for nomadic and fixed terminals, respectively. The relatively recent HSDPA standard proposal [1] aims at alleviating this shortcoming, especially on the downlink where most of the asymmetric data traffic is expected, by allowing implementation of enhanced receiver technologies that boost transmission rates up to multiple Mb/s. Among these techniques we underline space-time processing, multi-user detection, MIMO, space-time coding (STC), and adaptive modulation and coding [2],[3].

We have previously developed STAR, a new CDMA receiver that significantly outperforms the conventional RAKE in spectrum efficiency [4]. Recently, we upgraded it from a single-user receiver to a multi-user detector called interference subspace projection (ISR) [5]. More recently we have developed a very efficient version of STAR-ISR for the downlink that integrates MIMO and space-time coding [6]. The resulting enhanced receiver structure readily enables a peak rate of 512 Kb/s per spreading code with BPSK (with 4 spreading factor and 1/2 coding rate in 5 MHz) [5].

In order to achieve even higher peak rates, we propose new improvements of STAR [4] that allow its operation using higher-order M-PSK and M-QAM modulations with or without power control, and both in the blind mode with differential modulation or in the reference-assisted mode with new pilot use [7]. We also incorporate the resulting high-order-modulation STAR (HOM-STAR) in a transceiver structure that operates with both convolutional or turbo codecs. For simplicity of the structure, neither adaptive coding-rate nor trellis-coded modulation are supported. We define instead decoding metrics that allow implementation of adaptive modulation with the same convolutional or turbo codec. In order to allow an effective rate control for adaptive modulation and maximize throughput with HOM-STAR, we propose the use of power control (PC) jointly with two new rate allocation schemes (RAS). Both amount to imposing different received power levels that reflect the rates required according to the user profile (UP-RAS) or location (UL-RAS), in contrast to the currently popular rate allocation schemes that rely on the channel state (CS-RAS) [8].

THE WORK REPORTED HERE WAS SUPPORTED BY A CANADA RESEARCH CHAIR IN HIGH-SPEED WIRELESS COMMUNICATIONS AND BY THE STRATEGIC GRANTS PROGRAM OF NSERC.

Link-level simulation results suggest that high-order modulations up to 256QAM can be accommodated by HOM-STAR with use of turbo codes and 4 receive antennas, thereby enabling a peak rate of 768 Kb/s per spreading code with a processing gain of 32 and a coding rate of 1/2 in 5 MHz bandwidth. Higher peak rates can be readily attained with lower processing gains [5], more transmit antennas [6], multi-code or multi-carrier [9] transmission. System-level simulation results at a load of 20 users per cell or sector suggest that HOM-STAR with UP-RAS and UL-RAS offers an average throughput of 120-140 Kb/s on the uplink, i.e., an increase of about 100% over conventional CS-RAS.

2. DATA MODEL AND ASSUMPTIONS

For simplicity of presentation, we integrate high-order M-PSK and M-QAM modulations on the uplink of the single-user receiver STAR, although use of higher-order modulations is specified in HSDPA only [1]. Our investigation is directed to the uplink first because application there is simpler and will be extended to the downlink in the future. Furthermore, HSUPA (high speed uplink packet access) has received little attention in standardization so far [10], but it is likely to recommend use of higher-order modulations on the uplink in the future. Accordingly, we assume that each base-station is equipped with M uplink receiving antennas. At the mobile transmitter, the turbo-coded binary data sequence is first sliced and mapped onto a symbol sequence b_n belonging to a set of M-PSK or M-QAM constellation symbols $C_{\mathbb{M}} = \{c_1, \ldots, c_{\mathbb{M}}\}$, then spread by a long PN code with a processing gain $L = T_s/T_c$ where $R_b = 1/T_b$ and $R_c = 1/T_c$ denote the symbol and chip rates, respectively, before up-conversion and transmission over a multipath Rayleigh-fading channel. At the base-station receiver, the $ML \times 1$ post-correlation observation vector resulting from down-conversion, despreading, chip-rate sampling, symbol-rate framing and vector reshaping is [4]:

$$\underline{Z}_n = \underline{H}_n \quad {}_n b_n + \underline{N}_n = \underline{H}_n s_n + \underline{N}_n \ , \tag{1}$$

where $s_n = \quad {}_n b_n$ is the signal component, $\quad {}^2_n$ is the total received power, $\underline{H}_n$ is the $ML \times 1$ spatio-temporal channel vector and $\underline{N}_n$ is the $ML \times 1$ spatio-temporal noise vector.

3. HIGH-ORDER-MODULATION RECEIVER

3.1 General Structure

We provide below the general structure of HOM-STAR before we detail in the following subsections upgrades of STAR more specific to the HOM case. Provided that an estimate of the channel vector $\hat{\underline{H}}_n$ is available at symbol iteration n (as explained shortly), we first estimate the signal component by soft-decision MRC combining (see upgrade to ISR combining in [6]) as:

$$\tilde{s}_n = \frac{\hat{\underline{H}}_n^H \underline{Z}_n}{M} \ , \tag{2}$$

then extract the symbol estimate by hard decision as:

$$\hat{b}_n = \arg_{c_k \in C_{\mathbb{M}}} \min \| \tilde{s}_n - \hat{} \ {}_n c_k \|^2 \ , \tag{3}$$

where $\hat{}_n^2$ is the received power estimate (see sec. 3.3). Symbol estimation allows update of the channel estimate by decision feedback identification (DFI) [4] as:

$$\tilde{\underline{H}}_{n+1} = \hat{\underline{H}}_n + \quad (\underline{Z}_n - \hat{\underline{H}}_n \hat{s}_n)\hat{s}_n^* , \tag{4}$$

where is an adaptation step-size and $\hat{s}_n = \hat{}_n \hat{b}_n$. An analysis/synthesis step that exploits the temporal structure of the channel extracts the multipath time-delays (i.e., synchronization) from the coarse channel estimate $\tilde{\underline{H}}_{n+1}$ to reconstruct a far more accurate one $\hat{\underline{H}}_{n+1}$ (see details in [4] and references therein).

The DFI procedure above enables a blind version of HOM-STAR to estimate the symbols $\hat{b}_n$ within a phase ambiguity $r_k = e^{j\ k}$ (i.e., $\hat{b}_n \simeq r_k b_n$) that belongs to a limited set of rotations $R_{\mathbb{IM}}$[1] by which the constellation set $C_{\mathbb{IM}}$ remains invariant (i.e., $r_k c_{k'} \in C_{\mathbb{IM}}\ \forall c_{k'} \in C_{\mathbb{IM}}$). Hence, blind HOM-STAR applies only to differential IM-PSK (or star IM-QAM) and therefore transmits to the turbo decoder the differentially-detected soft-decision variable $d_n = \tilde{s}_n \tilde{s}_{n-1}^*$.

3.2 Pilot-Assisted Coherent Detection of IM-PSK & IM-QAM

In order to support coherent detection of both IM-PSK and IM-QAM modulations, we resort to the new pilot use proposed in [7] for BPSK and extend it to high-order modulation. The pilot-assisted HOM-STAR still identifies the channel blindly within a phase ambiguity using the above DFI procedure. However, from the pilot symbols (i.e., $b_n = 1$) it estimates the phase ambiguity $\hat{a}_{qA+n'}$ over the q-th block of A symbols as follows for $n' = 0, \ldots, A-1$:

$$\hat{a}_{qA+n'} = \arg_{r_k \in R_{\mathbb{IM}}} \min \left\| \sum_{l \in \ (q)} \frac{\tilde{s}_l}{card[\ \ (q)]} - r_k \right\|^2 , \tag{5}$$

where (q) and $card[\ \ (q)] = \ ^2A$ denote the set of pilot-symbol indices in the q-th block of A data symbols and its size, respectively. Note that the new pilot use for ambiguity resolution instead of conventional direct channel identification allows significant reduction of the pilot symbol overhead ^{2} [7]. Finally, pilot-assisted HOM-STAR transmits to the turbo decoder the coherently-detected soft-decision variable $d_n = \hat{a}_n \tilde{s}_n$.

3.3 Power Estimation and Control

The signal and noise power estimates are required to calculate and feed the LLRs to the turbo decoder as well as for power control (PC). If the latter is active, then these estimates are given by:

$$\hat{}_{n+1}^2 = (1 - \ \ )\ \hat{}_n^2 + \quad \mathrm{Re}\left\{\tilde{s}_n \hat{b}_n^* / |\hat{b}_n|\right\}^2 , \tag{6}$$

$$\hat{}_N^2 = (1 - \ \ )\ \hat{}_N^2 + \quad 2M\ \mathrm{Im}\left\{\tilde{s}_n \hat{b}_n^* / |\hat{b}_n|\right\}^2 , \tag{7}$$

where $\ll 1$ is a smoothing factor. If PC is not active, then smoothing of $\mathrm{Re}\left\{\tilde{s}_n \hat{b}_n^* / |\hat{b}_n|\right\}$ and $\mathrm{Im}\left\{\tilde{s}_n \hat{b}_n^* / |\hat{b}_n|\right\}$ is run over the pilot symbols only.

3.4 Channel Decoding Metrics

For simplicity of the structure, neither adaptive coding-rate nor trellis-coded modulation are supported. We define instead decoding metrics that allow operation of both blind and pilot-assisted HOM-STAR with the same convolutional or turbo codec with a fixed coding rate r and constraint length K. Detailed results regarding this particular issue can be found in [11]. For lack of space, we only provide an example of the decoding metrics for 8PSK and D8PSK. From each soft-decision variable d_n, we form the following triplet of decoding metrics:

$$\left[x_n^1, x_n^2, x_n^3\right] = \left[\mathrm{Re}\left\{\frac{d_n}{\hat{}_n}\right\}, \mathrm{Im}\left\{\frac{d_n}{\hat{}_n}\right\}, \left|\mathrm{Re}\left\{\frac{d_n}{\hat{}_n}\right\}\right| - \left|\mathrm{Im}\left\{\frac{d_n}{\hat{}_n}\right\}\right|\right].$$

[1] With IM-PSK, $R_{\mathbb{IM}} = C_{\mathbb{IM}}$ if $1 \in C_{\mathbb{IM}}$. With IM-QAM, $R_{\mathbb{IM}} = \{\pm 1, \pm j\}$.

Parameter	Value	Comment
BW	5 MHz	channel bandwidth
f_c	1.9 GHz	carrier frequency
R_b	128 Kbaud	baud rate
L	32	spreading factor
M	4	number of Rx antennas
P	3	number of paths
$^{-2}_{p}$	(0, 0, 0) dB	multipath power profile
f_D	1.7 Hz	Doppler frequency
$\frac{d}{dt}$	0.046 ppm	time-delays drift
e	4	path-loss exponent
$_s$	8 dB	std of log-Normal shadowing
r	1/2	turbo-coding rate
K	5	constraint length
T_f	5 ms	frame duration
	0.22	RRC rolloff factor
N_c	17	number of RRC coeffs
^{2}	5%	pilot symbol overhead
f_{PC}	1600 Hz	PC update frequency
P_{PC}	±0.25 dB	PC adjustment
$_{PC}$	0.625 ms	PC feedback delay
BER_{PC}	5%	simulated PC BER
$\mathrm{PC}^{\max}_{\min}$	±30 dB	PC margin
$^{-2}_{i}$	(0,3,5,11,14) dB	received power levels
p_i	(5,25,30,30,10)%	allowed Rx power probs

Table 1: Parameters used in the simulations.

For IM-QAM, we define decoding metrics similar to those reported in [12] for 16QAM. With $r = 1/2$ coding rate, the decoder slices the sequence $\{\ldots, x_{n-1}^1, x_{n-1}^2, x_{n-1}^3, x_n^1, x_n^2, x_n^3, x_{n+1}^1, x_{n+1}^2, x_{n+1}^3, \ldots\}$ into metric pairs for channel decoding.

3.5 New Rate Allocation Schemes

High-order modulations find best use in variable-rate transmission using adaptive modulation schemes. The current popular view is to implement adaptive modulation without power control and to let the channel state (CS), i.e., the signal to noise ratio (SNR), decide the appropriate rate (i.e., modulation) to choose for throughput maximization [8]. In the following, we refer to this common adaptive modulation technique as CS-RAS (rate allocation scheme). It is desirable, however, to have control over the transmission rate instead of leaving it depend on the random propagation conditions. Power control is an efficient way to mitigate the gap in received power from different users due to fast fading, path loss and shadowing. Additionally, it can reduce the received power variations significantly and hence approach the Gaussian channel. Hence it acts as a virtual diversity source by which high link-level gains can be achieved. However, it tends to equalize the SNR among users and hence leaves the traffic load (TL) decide the appropriate and unique rate for throughput maximization. In the following, we refer to this new adaptive modulation technique as TL-RAS. In order to allow an effective rate control, we propose the use of PC jointly with two new rate allocation schemes. Both amount to imposing different received power levels $^{-2}_{i}$ that reflect the rates required according to the user profile or location:

1. The *user-profile-based* RAS (UP-RAS) imposes a time share for each power level $^{-2}_{i}$ with a given probability distribution p_i that reflects a desired traffic profile.
2. The *user-location-based* RAS (UL-RAS) imposes concentric zones[2] where mobiles located in the inner zones closer to the base station are allocated the highest power levels $^{-2}_{i}$ to limit the interference propagated to the neighboring cells.

[2] For fair comparisons, zones are dimensioned such that uniformly distributed mobiles in the cell reflect on average the required distribution p_i.

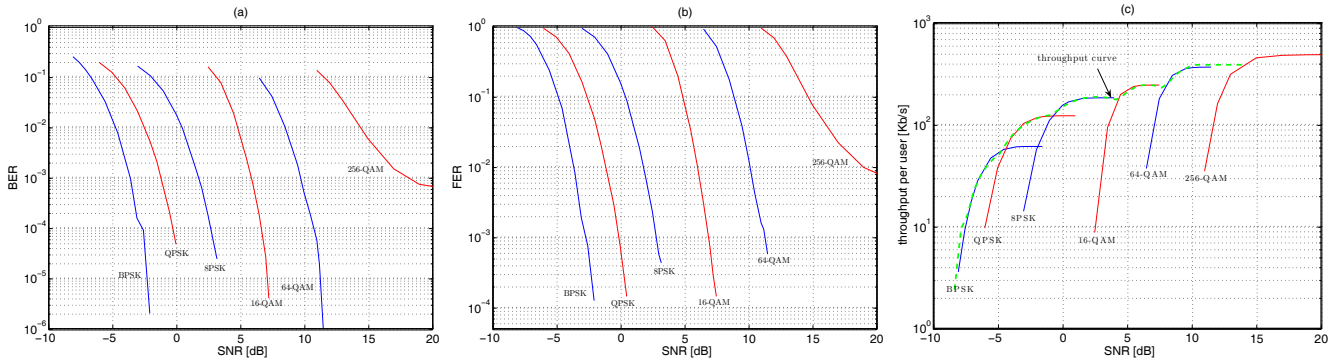

Figure 1: Link-level performance of HOM-STAR without PC versus SNR. (a): BER, (b): FER, and (c): throughput per user.

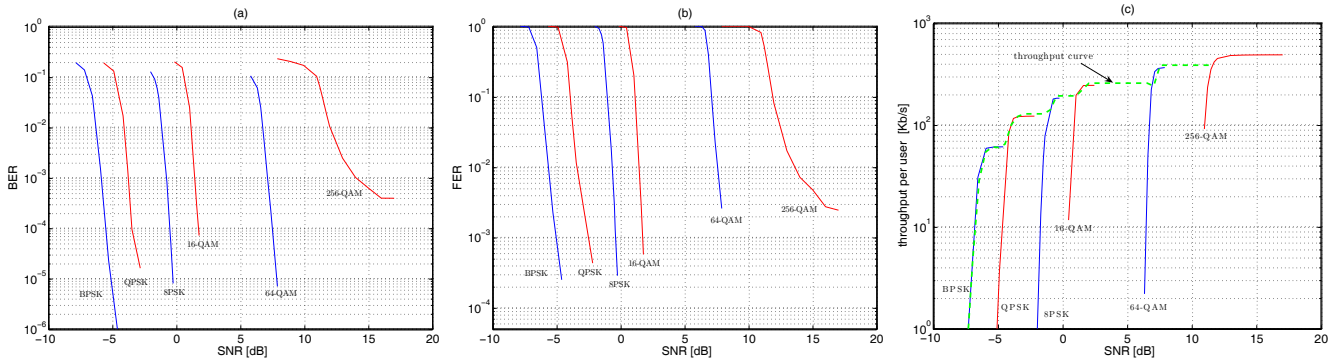

Figure 2: Link-level performance of HOM-STAR with PC versus SNR. (a): BER, (b): FER, and (c): throughput per user.

In the following, we evaluate the link-level performance of HOM-STAR with and without PC and its system-level performance with adaptive modulation and the four RAS described above.

4. SIMULATION RESULTS

All the setup parameters used in the simulations are listed in Tab. 1.

In Figs. 1 and 2, we provide the link-level results of HOM-STAR in terms of SER, FER, and throughput[3] versus SNR with and without PC, respectively. They suggest the following:

- HOM-STAR can accommodate up to 256QAM, i.e., 768 Kb/s per spreading code either with or without power control. Unlike other lower-order modulations, however, 256QAM shows a saturation at high SNR both in SER and FER due to increasing imperfections in channel and power estimation. For simplicity, we discard 256QAM from the system-level simulations below.
- In contrast to previous results reported in the literature [13] and in the standards [1], where 8PSK and 16QAM were found to require about the same SNR, we find that 8PSK offers a significant SNR gain of about 2.5 dB relative to 16QAM with or without PC, closer to the gap expected from theory. More generally, the SNR gaps we find between the different modulations better reflect the theoretical ones, thereby showing the near-optimality of the new HOM-STAR receiver.
- The implementation of PC results in large SNR gains (at a given BER or FER) with all modulations that translate into a significant increase in link-level throughput per user with adaptive modulation.

We translate the link-level results above to the system-level by a simulation tool that: 1) uniformly populates a grid of cells with mobile users up to the required capacity per cell or sector, 2) fixes the transmission rate and power of each user according to the selected RAS (see sec. 3.5), and 3) measures the resulting SNR and throughput (see footnote 3). In Figs. 3 and 4, we provide the system-level results of HOM-STAR in terms of throughput statistics and rate allocation probabilities. They suggest the following:

- TL-RAS performs best in terms of throughput statistics while conventional CS-RAS performs worst. This result translates the net advantage of implementing PC.
- UP-RAS and UL-RAS perform a little bit worse than TL-RAS in terms of throughput statistics, but much better than conventional CS-RAS. They suggest that PC-controlled SNR gaps result in higher throughput than those resulting from random channel realizations.
- The loss in throughput of UP-RAS and UL-RAS versus TL-RAS is traded for a better control of rate allocation. Indeed, Fig. 4 suggests that the rate allocation probabilities for UP-RAS and UL-RAS are different from those generated by TL-RAS and CS-RAS. CS-RAS shows that BPSK increasingly dominates as the load increases. TL-RAS shows that each rate fits best for a given load region (16QAM, 8PSK, QPSK dominate at around 7, 17 and 30 users per cell or sector). On the other hand, UP-RAS and UL-RAS suggest that high rates can be allocated even at high loads.
- UL-RAS slightly outperforms UP-RAS. This result underlines the advantage of restricting high-speed transmissions with high-order modulations (the most interfering links) to the inner zones closer to the base-station.
- At a load of 20 users per cell or sector, UP-RAS, UL-TAS and TL-RAS more than double the average throughput per user (i.e., 120-160 Kb/s vs 60 Kb/s) and the average total throughput per cell or sector (i.e., 2.3-3.1 Mb/s vs. 1.25 Mb/s) of conventional CS-RAS.

Ongoing research work investigates a hybrid RAS that allows a different user-profile in each zone with the peak power allocation probability increasing closer to the base-station, thereby allowing more fairness in access to high speeds in each cell while limiting their interference to the adjacent ones. In parallel, we are extending this work to a HOM multi-user detector with MIMO and STC. We will report on these studies in future publications.

[3] We assume packet transmission and ARQ. The dashed-line curve obtained by interpolation provides the system-level evaluation tool with an analytical expression for the calculation of throughput versus SNR.

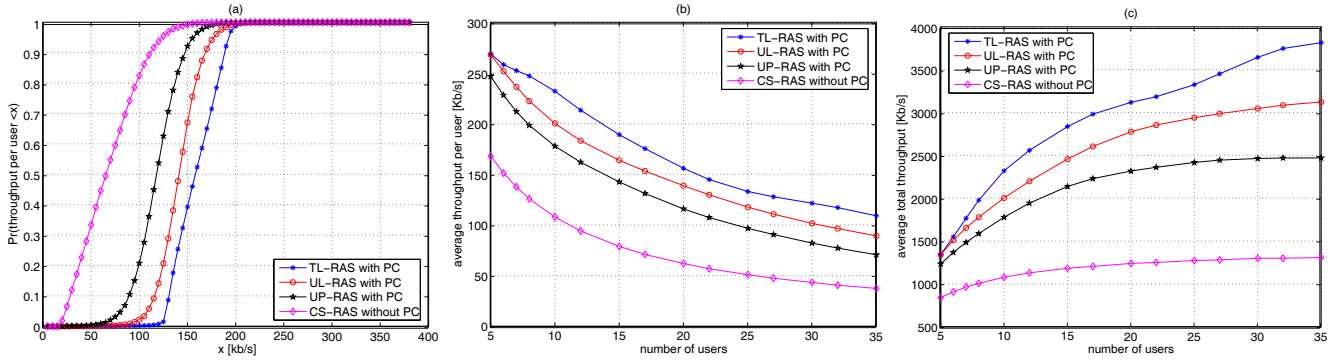

Figure 3: System-level performance of HOM-STAR with/without PC and different RAS options. (a): CDF of throughput per user for 20 users per cell or sector, (b): average throughput per user versus cell or sector load, and (c): average total throughput versus cell or sector load.

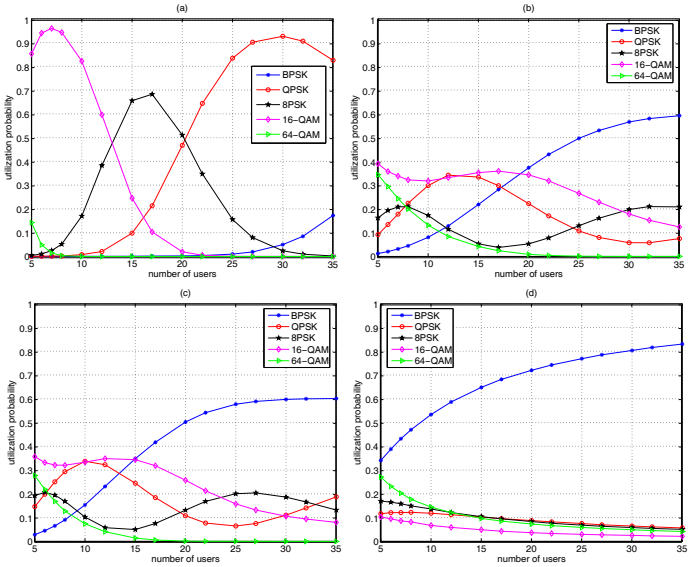

Figure 4: Rate utilization probability of HOM-STAR using (a): TL-RAS, (b): UL-RAS, (c): UP-RAS, and (d): CS-RAS.

5. CONCLUSIONS

In this work, we introduced improvements to the spatio-temporal array-receiver [4], a very promising wideband CDMA receiver, to allow its operation with IM-PSK & IM-QAM high-order modulations (HOM). The resulting HOM-STAR receiver operates both in the blind and pilot-assisted modes, with or without power control, and implements rate allocation schemes (RAS) jointly with power control (PC) that adapt to the user profile (UP) or location (UL). Link-level simulation results suggest that high-order modulations up to 256QAM can be accommodated by HOM-STAR with use of turbo codes and 4 receive antennas, thereby enabling a peak rate of 768 Kb/s per spreading code with a processing gain of 32 and a coding rate of 1/2 in 5 MHz bandwidth. Higher peak rates can be readily attained with lower processing gains [5], more transmit antennas [6], multi-code or multi-carrier [9] transmission. System-level simulation results at a load of 20 users per cell or sector suggest that HOM-STAR with UP-RAS and UL-RAS offers an average throughput of 120-140 Kb/s on the uplink, i.e., an increase of about 100% over conventional rate allocation schemes based on channel state.

6. ACKNOWLEDGMENT

The authors would like to thank Dr Jianming Wu from Nortel Networks for his helpful comments on the system-level simulation methodology and results.

REFERENCES

[1] 3GPP, TSG, RAN, *Physical Layer Aspects of UTRA High Speed Downlink Packet Access*, 3GPP TR 25.848, V4.0.0, 2001.

[2] L. Hanzo, C.H. Wong, and M.S. Yee, *Adaptive wireless transceivers: turbo-coded, turbo-equalized and space-time coded TDMA, CDMA and OFDM systems*, John Wiley & Sons, 2002.

[3] L. Hanzo, L.L. Yang, E.L. Kuan, and K. Yen, *Single- and multi-carrier DS-CDMA: multi-user detection, space-time spreading, synchronisation, standards and networking*, John Wiley & Sons, 2003.

[4] K. Cheikhrouhou, S. Affes, and P. Mermelstein, "Impact of Synchronization on Performance of Enhanced Array-Receivers in Wideband CDMA Networks", *IEEE J. Selec. Areas Comm.*, vol. 19, no. 12, pp. 2462-2476, December 2001.

[5] S. Affes, K. Cheikhrouhou, and P. Mermelstein, "Enhanced Interference Suppression for Spectrum-Efficient High Data-Rate Transmissions over Wideband CDMA Networks", *Proc. of IEEE ICASSP'03*, 2003, vol. IV, pp. 469-472.

[6] H. Hansen, S. Affes, and P. Mermelstein, "High Capacity Downlink Transmission with MIMO Interference Subspace Rejection in Multicellular CDMA Networks", *EURASIP Journal on Applied Signal Processing*, vol. 2004, no. 5, pp. 707-726, May 2004.

[7] S. Affes, N. Kandil, and P. Mermelstein, "Efficient Use of Pilot Signals in Wideband CDMA Array-Receivers", *Proc. of IEEE ICC'03*, 2003, vol. 4, pp. 2526-2531.

[8] I. Koffman and V. Roman, "Broadband Wireless Access Solutions Based on OFDM Access in IEEE 802.16", *IEEE Communications Magazine*, vol. 40, no. 4, pp. 96-103, April 2002.

[9] B. Smida, S. Affes, J. Li, and P. Mermelstein, "Multicarrier-CDMA STAR with Time and Frequency Synchronization", *Proc. of IEEE ICC'05*, 2005, to appear.

[10] IST-METRA Project, *Adaptive Modulation Schemes for MIMO HSDPA*, IST-2000-30148 IST-METRA, July 2002.

[11] F. Moatemri, *Amélioration de la Transmission de Données et de la Couverture sur les Réseaux WCDMA par des Récepteurs Spatio-Temporels à Modulation d'Ordre Supérieur*, MSc thesis (in french), Ref. M-763, 2003.

[12] S. Le Goff, A. Glavieux, and C. Berrou, "Turbo-Codes and High Spectral Efficiency Modulation", *Proc. of IEEE ICC'94*, 1994, pp. 645-649.

[13] L.M.A. Jalloul and A. Shanbhag, "Enhancing Data Throughput Using Quasi-Orthogonal Functions Aggregation for 3G", *Proc. of IEEE VTC'02-Spring*, vol. 4, pp. 2008 -2012.